IN SITU EXPERIMENTS ON THE GROWTH & TEXTURAL DEVELOPMENT OF SUBAERIAL MICROSTROMATOLITES, CHAMPAGNE POOL, WAIOTAPU, NZ

K. M. HANDLEY', K. A. CAMPBELL', B. W. MOUNTAIN[2] & P. R. L. BROWNE'

'Department of Geology, University of Auckland, Private Bag 92019, Auckland, NZ
[2]Institute of Geological and Nuclear Sciences, Wairakei Research Centre, Taupo, NZ

SUMMARY – Potential origins for a range of common silica sinter fabrics are evident from a continuing study of experimentally grown microstromatolites at Champagne Pool. Periodic collection of these actively accreting subaerial deposits provides incremental windows into the key stages of textural development. The results have particular significance for the formation of analogous spicular and finely laminated subaerial sinters formed by hydrodynamic mechanisms of surge, splash or wave action. At Champagne Pool, vitreous, granular, and filamentous-network sinter fabrics result from the silicification of bacterial filaments and, to a certain extent, vitreous and granular fabrics also form abiotically. External silicification of filaments is typically accompanied by rapid intracellular infill, resulting in loss of evidence of a biotic origin for porous and vitreous sinter fabrics. Transitions between alternating vitreous-porous laminae may be induced by variations in the supply of silica-charged waters, i.e. limited by periods of low wave action, yielding a filament-based porous, granular fabric. Vitreous laminae form where subaerial silica supply matches or exceeds growth rate of filament networks. Consequently, a decrease or increase in wave action may result in vitreous-porous or porous-vitreous transitions, respectively. Alternatively the formation of thin silica crusts derived from progressive silicification of films of mucilaginous exopolymeric substances, which drape and bridge topographies, create a barrier against further silica input. Hence silica crusts cause transitions in fabric types or promote the formation of fenestrae.

1. INTRODUCTION AND SETTING

Many of the textures of stromatolitic sinter fabrics are attributed to the presence of microorganisms and associated mucilaginous exopolymeric substances (EPS), which act as templates for mineralisation (Urmtia and Beveridge 1993; Westall et al. 1995; Campbell et al. 2001, 2002). Stromatolitic sinters commonly consist of alternating vitreous-porous laminae (e.g. Cady and Farmer 1996; Campbell et al. 2001). Laminae typically are interspersed with, or separated by, fenestrae (e.g. Konhauser et al. 1999; Campbell et al. 2001). Furthermore, it is common for such sinter fabrics to be classed as abiotic-biotic (e.g. Cady and Farmer 1996; Konhauser et al. 1999; Mountain et al. 2002). Alternating laminae couplets (i.e. vitreous-porous or abiotic-biotic) have been attributed to microenvironmental fluctuations in hydrodynamics or physicochemical parameters (Cady and Farmer 1996), or to seasonal effects on fluid composition (Hinman and Lindstrom 1996) or biota (Konhauser et al. 1999). The origin of fenestrae in stromatolitic sinters is enigmatic, except for the occurrence of photosynthetically derived gas bubbles in thick microbial mats (see refs. in Campbell et al. 2001).

This study is part of an ongoing investigation of possible abiotic and biotic mechanisms for primary sinter fabric formation. Textural studies are based upon subaerial microstromatolitic sinter that has been experimentally grown within Champagne Pool, Waiotapu. Sample material has accreted onto artificial substrates along a northern section of the pool, on a portion of subaqueous ledge that is ~ 10 cm deep and up to 250 cm wide, which parallels the natural raised sinter rim that encircles the pool. This sinter rim bristles with a moist fringe of conical microstromatolitic spicules, forming upon an overhanging ledge, and reaching up to 3 cm above water level. Jones et al. (1997) and Mountain et al. (2002, 2003) have previously described the sinter rim macroscopically and in part at the ultrastructural scale. Champagne Pool itself is a subcircular, chloride hot spring, pH 5.5 and approximately 65 m in diameter (Mountain et al. 2003). The pH indicates that silica is likely to be present in monomeric form (Brown and McDowell 1983). The temperature of the pool water is essentially constant at 75°C due to vigorous convection. The waters are therefore over-saturated with respect to amorphous silica at 430 mg kg^{-1} SiO_2 (Mountain et al. 2003).

3. METHODS

Experimental Design & Sample Collection

Subaerial sinter accumulated upon partially submerged glass microscope slides fixed to weighted subaqueous racks following Mountain et al. (2002, 2003). The use of artificial substrates affords precise control over the ages of deposits, and the correlation of growth rates and stratigraphic development with weather conditions that may influence microstromatolite formation. Periodic collections provide windows into incremental stages of the sinter development,

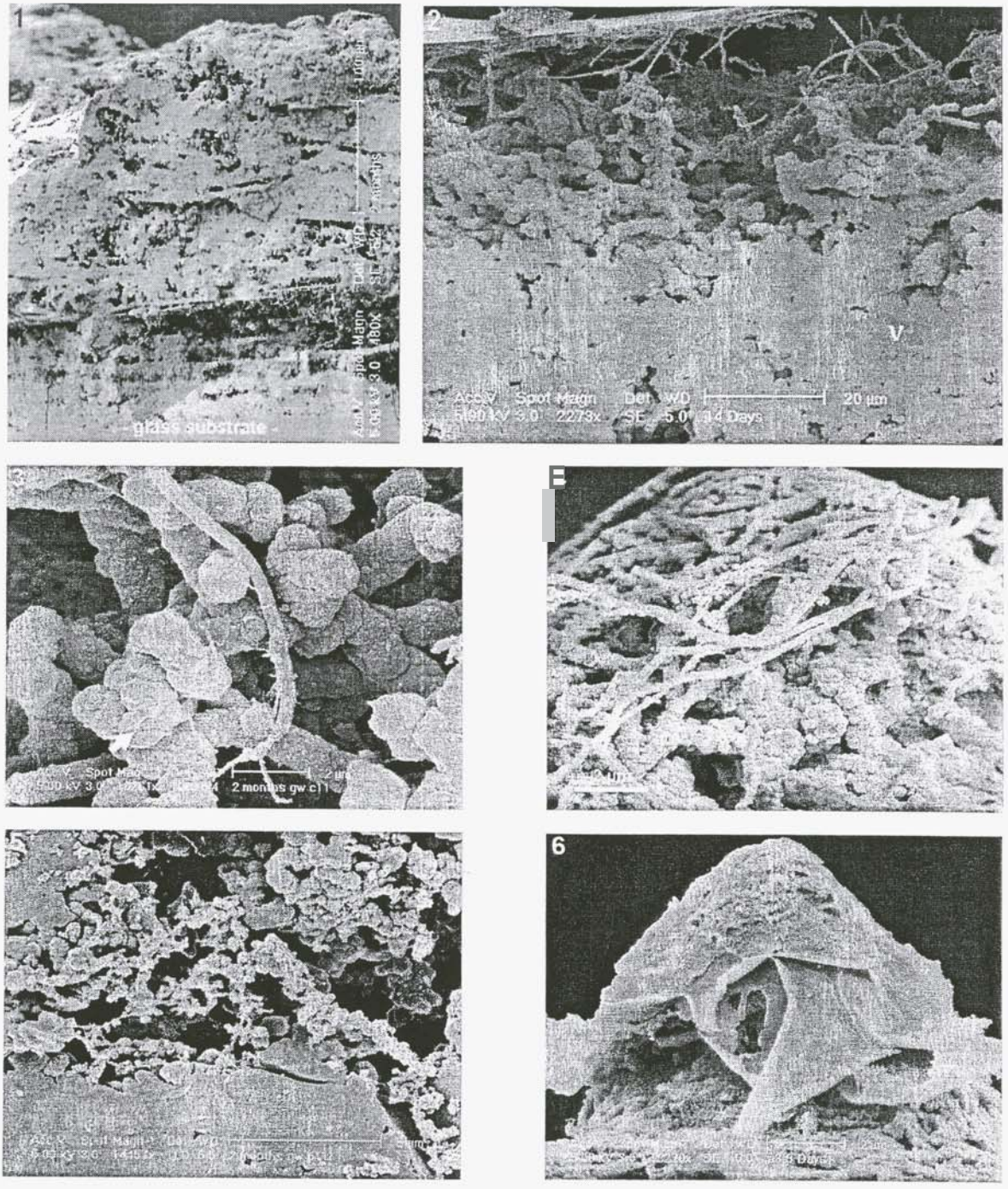

Figures: 1. Stratigraphic cross-section of two-months growth displaying vitreous, granular, filamentous-network, microspicular, and fenestrate sinter textures. 2. Filament-lined fenestra beneath a 1.5 µm thick silica crust. Vitreous sinter (v) formed by silica infill of silicified filament network interstices. 3. Filaments completely replaced by vitreous silica, with instances of rare internal tubes (– 100 nm) (arrow). Unsilicified, later-stage filament (400 nm) and EPS fibres (centre). 4. Microspicule of unsilicified (upper) to heavily encrusted (lower) filaments and EPS fibres. 5. Early-stage, loosely-packed granular sinter fabric with silica encrusted EPS fibres (< 100 nm unsilicified). 6. Microspicule draped in layers of lightly silicified EPS films. 7. Microspicule covered in silica crusts. Re-colonisation of the tip by fresh filaments.

and reveal key exposures at the surface of deposits for a variety of partially formed or transient sinter fabrics and textures that are soon obscured by further silicification. Samples collected over a two-month period have thus far been examined in detail. In addition, the effect of waves on silica accretion was determined by placing a plastic barrier around half a contingent of glass slides for daily collection over a three-day period. Wave crest heights, within the range of subaerial silica accretion, were measured by two HOBO Event data loggers attached to two cables positioned at 1 cm and 1.5 cm above the air-water interface.

Sample Treatment

To identify sinter fabrics and microbe-silica relations at the ultrastructural level, 23 samples were examined **using** a **SEM** fitted with a Phillips XL30S Field Emission Gun. Samples were therefore stored in 2.5% glutaraldehyde immediately upon collection in order to preserve the delicate structures of biological material. Sinter-bearing glass slides were snapped to obtain cross-sections through the vertical extent of the subaerial sinter deposits. To prevent the structural collapse and distortion that occurs when structurally bound water sublimates from hydrated biologic material within the vacuum chamber, samples were dehydrated using an E3000 Series 2 Polaron critical-point drier. First, samples were rinsed in deionised water and then dehydrated through an ethanol series. Ethanol was exchanged for liquid CO_2 by flushing and soaking for one hour before vaporising the liquid CO_2. Each sample was sputter-coated with gold-palladium or platinum (2-10 nm thick). A SiLi (Lithium drifted) EDS with a Super Ultra Thin Window was used to confirm the pervasive presence of silica.

4. RESULTS

Sinter Development & Textures

A complex sinter stratigraphy, with numerous continuous and discontinuous laminae, has formed by two months (Fig. 1). However, excluding microspicules, all common sinter fabrics and biologic attributes may become well-established within only a one-day period. Well-defined microspicules (≤ 30 µm high) formed in two days time. The main sinter fabrics and textures are dense non-porous vitreous, granular, filamentous-network, microspicular, and fenestrate (Figs. 1-7). EPS films (cf. surface mucilage of Paterson 1995) (Fig. *6)* and thin vitreous silica crusts (Fig. 2) also are common at the surface of deposits. Granular sinter ranges from loosely-packed and chain-like irregular spheres (Figs. **4,** 5) to densely-packed and structureless. Granular laminae, vitreous laminae, and fenestrae (voids) are laterally continuous in cross-section. Thin, laterally continuous vitreous laminae (~ 1-5 µm thick) tend to be non-fenestrate, while thick vitreous laminae (~ 10-50 µm thick) are interrupted to widely varying degrees by: (1) fenestrae of irregular distribution, shape, and size (submicron to tens of microns), (2) granular silica in filled pockets or as discontinuous sub-laminae, and **(3)** wind-blown diatom tests. Fenestrae linings in vitreous sinter may be smooth, filamentous, or granular. Fenestrae also occur in granular or filamentous-network fabrics. Contacts between laminae are typically sharp, or rarely gradational, representing rapid changes in conditions affecting subaerial or subsurface silica supply. These contacts may be wavy, undulating, or irregular due to a spicular paleotopography, or planar where they overlie flat, non-spicular surfaces.

Cross-sections of deposits revealed that, by six hours growth, a predominantly vitreous sinter fabric prevails (≤ 10 µm thick). After only one hour of growth, accreted sinter varies from largely abiotic in appearance to highly filamentous, with associated EPS fibres, films and matrices. Sinter establishes itself in an extensive band or as discrete clumps. Sinter fabrics are either: (1) smooth and vitreous, or (2) comprise densely-packed opal-A nanospheres (≤ 100 **nm)** and/or microspheres (in ≤ 250 nm or ≤ 1 µm diameter sizes) (cf. Rodgers et al. 2002). Commonly these microspheres coalesce at the necks, emulating the frog-spawn habit identified by Rodgers et al. (2002) in silica residue deposits. Deposits of six hours, and those of one to five days growth, each revealed a predominantly vitreous deposit with little to no biotic aspects identifiable by SEM. However, the top surface of each of these samples is extensively strewn with prostrate filaments and three-dimensional filament networks that are interspersed with filamentous microspicules (≤ 30 µm high) at varying stages of silicification. **As** each of these surfaces represents an increment in sequential growth, it is clear that apparently abiotic vitreous sinter therefore has a biotic template. Furthermore, a range of samples reveals that silicified filaments appear to be solid vitreous silica in cross-section, and display no evidence of any distinct or extracellular layers. Rarely do silica-encrusted filaments present hollow moulds in cross-section (100-200 nm internal diameters).

Microspicules are erect, conical structures constituting silicified networks of intertwined filaments (Figs. **4, *6,* 7).** Each spicule develops from a growing colony of bacterial filaments. Filaments are unbranched, and when unsilicified are typically of two diameters, 250 nm (Fig. **4)** and 400 nm (Fig. **3).** Nonetheless larger filaments of up **to** 2 µm in diameter also are common where deposits form on the tops of slides less than ~ 1 cm above water level, owing

to as yet unknown reasons. Notably silica also is accreted at a greater rate on the tops of these slides, e.g. 350 µm *versus* 100 µm accumulation in two months. Microstromatolite surface topographies range from highly irregular to regular, depending upon the consistency of microspicule distributions and sizes. The topography and size-range both increase with the age of the sample, as certain microspicules excel in growth, whereas others are smothered in silica, discontinued, and then new growth centres emerge (Fig. 7). Microspicule and non-spicular filament networks have bases typically comprised of vitreous laminae that may have been the foundation upon which the microspicule first established, or may have resulted from silica infilling the filament network interstices (Fig. 2). Often there is a trend of increased silicification towards the base (Figs. 2, 4), although this trend also may be inverted or lateral, indicating an increase in silica supply or lateral filament growth, respectively. Filaments may be unsilicified, or are visibly coated in a smooth to very fine granular texture of opal-A nanospheres (≤ 100 nm) that coalesce as the silica encrustation thickens. A distinct granular texture is imparted to filaments where opal-A microspheres (≤ 250 nm) contribute to the encrustation. Associated EPS fibres also are silicified, commencing with a granular encrustation of fibres by opal-A nanospheres (≤ 50-100 nm), and later accompanied by microsphere (≤ 250 nm) deposition (cf. Westall et al. 1995). Filaments and EPS fibres that are heavily encrusted in granular silica form a granular fabric of chain-like morphology (Figs. **4,** 5). More densely-packed granular fabrics become structureless, and no longer display any physical evidence of their biotic origin. Structureless, granular sinter fabrics consist of unclustered or evenly-sized clusters of nanospheres and microspheres.

Filament networks are commonly associated with **EPS** fibres, extensive or discontinuous films of mucilaginous EPS, or thin EPS-derived silica crusts. In particular, microspicules are often draped in singular or multiple layers of EPS films (Fig. 6), although these also may extend over areas that are sparse in unsilicified filaments. Films of EPS range from unsilicified through to heavily silicified and crust-like (Figs. *6,* 7). Lightly silicified EPS films are in some places smooth and continuous, but commonly they are tom and patchy due to desiccation and contraction. Heavily silicified examples of desiccated films indicate that this disruption of film integrity can be a natural pre-collection event, rather than due to sample preparation. In some instances, EPS fibres appear to have formed fkom films that have contracted, with the loose edges rolling inwards. Thin EPS-based crusts of smooth silica are common at the surface of deposits, due to the rapid silicification of EPS films. In some cases, silica crusts are directly overlain by an EPS film or a second silica crust. These crusts vary fi-om: (1) torn and/or folded sheets that drape the surface topography, to (2) curved and planar sheets that either extend over the surface topography with limited physical support from beneath, or with support from loosely-packed silicified-filament networks (Figs. 2, 7). In places, filaments line the underside of these crusts, beneath which fenestrae have formed (Fig. 7). Curved and planar crusts increase in thickness from < 100 nm to form micron-scale vitreous laminae. Vitreous laminae are typically planar, but thin laminae also may be curved. Of these fabrics, only vitreous laminae are present in the sinter subsurface; EPS films and silica crusts are found only on subaerial depositional surfaces.

Waves

Over a three-day initial study period (August 2003), silica accreted onto glass slides that were either sheltered or unsheltered from wave action. During this period, wave heights of between 1 and 1.5 cm were common. Wave action was observed to have subdued or nil effect on the sheltered slides. There was a significant difference between the subaerial silica accreted onto the sheltered and unsheltered slides: an opaque band of silica (2 µm thick after one day) formed on the unsheltered slides, while on sheltered slides a fine film of transparent silica (≤ *6* µm thick) formed a semi-opaque layer.

5. DISCUSSION

Various mechanisms have been suggested for the transport of silica and formation of subaerial sinter in hot spring settings. Subaerial silica may be supplied by hydrodynamic means: splash, surge, and wave action (Jones et al. 1997; Braunstein 1999). Also important are water-tension effects: meniscoid and capillary creep (Hinman and Lindstrom 1996; Jones et al. 1997; Campbell et al. 2002; Mountain et al. 2003). Silica accretion experiments in this study have confirmed that silica is primarily supplied to subaerial substrates in Champagne Pool by wave action, as proposed by Jones et al. (1997) and Mountain et al. (2002, 2003). The rate of subaerial sinter accreted at Champagne Pool is therefore strongly dependent upon wind conditions contemporaneous with growth. However, wave borne silica supplies also are supplemented by capillary creep, particularly after a porous path through initial sulphur and silica grains has been well-established subaerially down to the air-water interface.

Transitions in sinter fabric-types result from changes in silica supply to the outer surface of microstromatolites, either caused by

impenetrable silica crust development, or variations in wave action. Silica-charged water is excluded from microstromatolite surfaces by patchy, overlying thin crusts of silicified EPS films that drape the surface. Porous sinter fabrics are therefore preserved in the subsurface of the deposit wherever these silica crusts prevent further silicification. Accordingly, preservation of filamentous-network fabrics, chain-like granular fabrics, densely-packed structureless granular fabrics, or clusters of small fenestrae in vitreous sinter depends upon the degree of filament network silicification at the time of crust formation. Fenestrae also are created where silica crusts bridge topographic highs, or drape unsilicified filament networks that subsequently degrade. These latter fenestrae may be laterally discontinuous, occurring over a wide range of shapes and sizes, or have planar geometries between vitreous laminae. Fenestrae also probably form due to the irregular interstices and hence non-uniform permeability of filament networks, whereby silica rapidly infills spaces amongst closely arranged filaments, and could therefore preclude silica-bearing waters from adjacent interstices. Increases or decreases in wave action, and hence also subaerial silica supply, can result in transitions between vitreous and porous laminae (cf. Cady and Farmer 1996). In periods of low wave action, a porous lamina of filamentous or granular sinter may build-up where filament growth exceeds the rate of vitreous deposit formation. Conversely a subsequent increase in wave activity, such that the subaerial silica supply is not exceeded by filament growth, likely results in a transition fkom porous to vitreous sinter. Where filaments are inundated by silica or where silica crusts drape microstromatolite surfaces, a thin band of largely abiotic vitreous sinter may form if the rate of silica supplied by wave action exceeds the rate of filament repopulation. The re-establishment of filaments on surfaces draped in EPS films, silica crusts or vitreous laminae may result in: (1) the re-establishment of EPS films and hence formation of biogenic silica crusts, (2) sufficient filament build-up in calm conditions for a vitreous-porous laminae transition to occur, or (3) continued build-up of the vitreous laminae into a thick vitreous deposit of silicified filaments.

Factors influencing the deposition of subaerial hot spring sinters have been attributed to both abiotic and biotic mechanisms (Farmer 1999). Precipitation of the Champagne Pool subaerial sinter is most likely induced abiotically due to increased silica saturation resulting fiom cooling and evaporation (cf. Rimstidt and Cole 1983; Mountain et al. 2003). The silica supplied to the subaerial sinter is in monomeric form, and is therefore driven to polymerise and precipitate as the water evaporates. It appears that bacterial surfaces act as passive templates for silica deposition (cf. Urmtia and Beveridge 1993; Westall et al. 1995; Farmer 1999; Konhauser et al. 1999; Mountain et al. 2003). The silicification and potential preservation of bacteria and associated **EPS** is likely to proceed initially through hydrogen bonding between silicic acid and functional groups upon and within the EPS, bacterial cell walls and extracellular surface layers (cf. Urrutia and Beveridge 1993; Westall et al. 1995; Farmer 1999). Subsequent dehydration results in siloxane bond formation between the adsorbed silica and functional groups, followed by abiotic, homogeneous silica polymerisation. Polymerisation and aggregation in solution leads to the formation of juvenile opal-A nanospheres and then microspheres (cf. Smith et al. 2001). The coalescence of nanospheres and microspheres is due to precipitation of soluble silica and small spherules within the areas of negative radius and low interfacial energy at the necks of joined silica spheres (cf. Rimstidt and Cole **1983).** By this method of spherule deposition and cementation, silica progressively builds-up as densely-packed granular filament encrustations, and infills filament network interstices (Fig. 2). Where silica supply to the filament networks is unimpeded, a vitreous sinter fabric ultimately forms. Significantly the rate of sinter growth is greatly increased by the presence of three-dimensional networks filament. These networks, covering large proportions of microstromatolite surfaces, continually present fresh, self-replicating substrates of high surface area upon which silica can deposit. Hence, areas of higher topographic relief develop where the potential for filament encrustation and network interstice-infill is the greatest.

In most cases, filaments in the Champagne Pool subaerial microstromatolites are rapidly penetrated by silica and completely infilled. Only the general morphology of filaments is preserved in loosely-packed sinter fabrics, as viewed in SEM (Figs. 2, **3).** Cross-sections reveal that filaments are completely replaced by vitreous silica in the early stages of silicification. Therefore we cannot distinguish external surfaces. Furthermore, when interstices among adjacent filaments are completely infilled, vitreous sinter is formed, resulting in the complete obliteration of the bacterial form in SEM. In general, cell preservation appears less common in thermophiles, possibly due to a tendency towards smaller cell diameters and thinner (or lack **of)** extracellular layers, resulting in ease of silica penetration, and a greater susceptibility to obliteration during diagenesis (Farmer 1999). The sequential order of internal and external silicification of filaments is uncertain. However, the rapid rate of filament silicification indicates that intracellular

silicification is probably not a secondary process, but may pre-empt (cf. Westall et al. 1995) or occur concurrently with the formation of a visible granular silica crust at the surface of the bacterium. In rare instances only encrustation of filaments has occurred, resulting in empty silica moulds. Here, lack of intracellular silicification is possibly caused by small variations in the rate of silicification of adjacent and similar filaments, whereby encrustation outpaces infiltration. Westall et al. (1995) found that in addition to the physicochemical conditions of mineralisation, the degree **of** structural preservation depends upon the type of bacteria (e.g. species or gram-type). Silica moulds therefore also' may form due to different bacterial populations, possessing extracellular layers or cell walls that are less permeable to silica. Ultimately, examination of samples by TEM **is** necessary to further elucidate the cellular structures and the processes involved in filament silicification.

6. ONGOING & FUTURE WORK

Continuing examination of sinter development in this study includes further analyses of sequential growth, and a comprehensive study of sinter ultrastructural textural variations and accretion with respect to wind and wave exposure effects. Wind speed, wind direction, and precipitation are being recorded by a weather station located in close proximity to Champagne Pool (~ 30 m).

7. ACKNOWLEDGMENTS

Thanks are due to **A.** Leinhardt and staff at Waiotapu for site access; and C. Hobbis, B. James, **A.** Turner, R. Sims, D. Graham, M. Muller, and L. Cotterall for technical assistance. Financial support was provided by the FRST Geothermal for the New Millenium Contract C05x0201, the NSOF Extremophiles Programme, and the Freeston Licensing Trust.

8. REFERENCES

Braunstein, D.G. **(1999)** ***The role of hydrodynamics in the structuring and growth of high-temperature (>73°C) siliceous sinter at neutral to alkaline hot springs and geysers, Yellowstone National Park.*** PhD dissertation, Stanford University **1-163.**

Brown, K.L. and McDowell, G.D. **(1983)** pH control of silica scaling. ***Proc. 5th NZ Geothermal Workshop*** **1-5.**

Cady, S.L. and Farmer, J.D. **(1996)** Fossilization processes in siliceous thermal springs: trends in preservation along thermal gradients. In: ***Evolution of hydrothermal ecosystems on Earth (and Mars?),*** G.R. Bock and J.A Goode (eds.), Wiley, Chichester **150-173.**

Campbell, K.A., Sannazzaro, K., Rodgers, K.A., Herdianita, N.R. and Browne, P.R.L. **(2001)** Sedimentary facies and mineralogy of the Late Pleistocene Umukuri silica sinter, Taupo Volcanic Zone, New Zealand. ***Journal of Sedimentary Research*** **71(5), 727-746.**

Campbell, **K.A.,** Rodgers, K.A., Brotheridge, J.M.A. and Browne, P.R.L. **(2002)** ***An*** unusual modem silica-carbonate sinter from Pavlova spring, Ngatamariki, New Zealand. ***Sedimentology*** **49, 835-854.**

Farmer, J. **(1999)** Taphonomic modes in microbial fossilization. In: ***Size limits of very small microorganisms,*** Proc. of a Workshop, Space Studies Board, Commission on Physical Sciences, Mathematics and Applications, NRC: National Academy Press, Washington **94-102.**

Hinman, N. **W.** and Lindstrom, R. F. **(1996)** Seasonal changes in silica deposition in hot spring systems. ***Chemical Geology*** **132,237-246.**

Jones B., Renaut, R.W. and Rosen, M.R. **(1997)** Vertical zonation of biota in microstromatolites associated with hot-springs, North Island, New Zealand. ***Palaios*** **12,220-236.**

Konhauser, K.O., Phoenix, V.R., Bottrell, S.H., Adams, D.G. and Head, I.M. **(1999)** Microbial-silica interactions in modern hot spring sinter. In: ***Geochemistry of the Earth's Surface,*** Balkema, Rotterdam **263-266.**

Mountain, B.W., Boerema, J. and Benning, L.G. **(2002)** Biomineralisation in New Zealand Geothermal Areas: **A** progress report. ***Proc. 24th NZ Geothermal Workshop*** **229-234.**

Mountain, **B.W.,** Benning, L.G. and Boerema, J.A. **(2003)** Experimental studies on New Zealand hot spring sinters: rates of growth and textural development. ***Canadian Journal of Earth Sciences*** (in press).

Paterson, D.M. **(1995)** Biogenic structure **of** early sediment fabric visualized by low-temperature scanning electron microscopy. ***Journal of the Geological Society, London*** **152, 131-140.**

Rimstidt, J.D. and Cole D.R. **(1983)** Geothermal Mineralization I: The mechanism of formation of the Beowawe, Nevada, siliceous sinter deposit. ***American Journal of Science*** **283, 861-875.**

Rodgers, K.A., Cook, K.L Browne, P.R.L. and Campbell, K.A. **(2002)** The mineralogy, texture and significance of silica derived from alteration by steam condensate in three New Zealand geothermal fields. ***Clay Minerals*** **37,299-322.**

Smith, B.Y., Rodgers, K.A. and Browne, P.R.L. (2001) Opal-A – the first **100** days. ***Proc. 23rd NZ Geothermal Workshop*** **131-136.**

Urrutia, M.M., and Beveridge, T.J. **(1993)** Mechanism of silicate binding to the bacterial cell wall in ***Bacillus subtilis. Journal of Bacteriology*** **175, 1936-1945.**

Westall, F., Boni, L. and Guerzoni, E. **(1995)** The experimental silicification of microorganisms. ***Palaeontology*** **38(3), 495-528.**